ELSEVIER

Journal of Power Sources 63 (1996) 47–51

JOURNAL OF POWER SOURCES

Fuel cells with doped lanthanum gallate electrolyte

Man Feng [a], John B. Goodenough [a], Keqin Huang [a], Christopher Milliken [b]

[a] *Center for Materials Science and Engineering, The University of Texas at Austin, Austin, TX 78712-1063, USA*

[b] *Ceramatec, Inc., 2425 South 900 West, Salt Lake City, UT 84 119, USA*

Received 2 April 1996; revised 11 June 1996

Abstract

Single cells with doped lanthanum gallate electrolyte material were constructed and tested from 600 to 800 °C. Both ceria and the electrolyte material were mixed with NiO powder respectively to form composite anodes. Doped lanthanum cobaltite was used exclusively as the cathode material. While high power density from the solid oxide fuel cells at 800 °C was achieved, our results clearly indicate that anode overpotential is the dominant factor in the power loss of the cells. Better anode materials and anode processing methods need to be found to fully utilize the high ionic conductivity of the doped lanthanum gallate and achieve higher power density at 800 °C from solid oxide fuel cells.

Keywords: Lanthanum gallate; Solid oxide fuel cells; Power density; Overpotential

1. Introduction

Solid oxide fuel cells offer an environmentally benign alternative to heat engines in generating electric power. Unrestrained by Carnot's law, fuel cells boast a high fuel efficiency. Low operating temperature (<800 °C) is not only important to achieve the projected high efficiency, but it is also essential to lower maintenance costs and to avoid significant corrosion on various parts of fuel cells. For the traditional electrolyte material, doped zirconia, systematic processing methods and successful model cells operating above 1000 °C have been developed. However, its relatively low ionic conductivity at 800 °C (~ 0.03 S/cm) made it an undesired candidate for the electrolyte, particularly in view of its marked aging effect between 600 and 900 °C.

Strontium and magnesium doped lanthanum gallate (LSGM) was identified as a superior oxide-ion conductor [1–4] with good chemical stability and no aging effects. Its conductivity at 800 °C is about the same as that of zirconia at 1000 °C. Therefore, LSGM is a primary candidate for constructing thin membrane ceramic fuel cells operating at 800 °C. We tested two fuel cells with this electrolyte with various composite anode materials. While a large open-circuit voltage (OCV) was achieved in these cells, a significant electrode overpotential was observed, particularly at the anode side. We report here on our experimental results.

PII S0378-7753(96)02441-X

2. Experimental

LSGM electrolyte materials were prepared by intimately mixing La_2O_3, Ga_2O_3, $SrCO_3$ and MgO. Several calcinations at 1250 °C were performed to make sure all starting materials are reacted. The product thus obtained contains $LaSrGaO_4$ impurity in addition to the main doped lanthanum gallate cubic phase. The powders were then milled in agate balls to reduce their particle size. Large round pellets were cold-pressed and sintered at 1550 °C for 6 h. The sintered pellets were ground with diamond wheels to reduce their thickness and surface roughness.

Single cells with LSGM electrolyte were then constructed. Doped lanthanum cobaltite ($La_{0.6}Sr_{0.4}CoO_{3-\delta}$) was selected as the cathode material because of its high conductivity to both electrons and oxide ions. For one cell, doped ceria mixed with an appropriate amount of NiO powder was used as the anode material. Ceria is partially reduced in the reducing atmosphere at the anode side of a fuel cell and become a mixed conductor to both electrons and oxide ions. Therefore, it is widely adopted as the supporting material in a composite catalytic anode. In another cell, a mixture of LSGM with NiO powder was used as the anode material because LSGM possesses a higher oxide-ion conductivity and is structurally more compatible with the electrolyte material. Reference electrodes with the same materials as those of corresponding working electrodes were also constructed for the monitoring

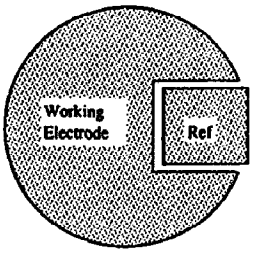

Fig. 1. Cell surface configuration.

of overpotentials on each electrode. The electrode materials were screen-printed on the surface of the electrolytes. After baking the printed electrolyte at 1130 °C overnight, platinum meshes were applied on the electrode surface as current collectors together with additional electrode paste to achieve good electric contacts. Fig. 1 displays the surface configuration for the fuel cells. The effective (electrode) areas of the electrolytes were 2.5 and 1.13 cm^2 for cells with ceria anode and LSGM anode, respectively. The thickness of the LSGM electrolyte was 0.265 and 0.395 mm, respectively. All the fuel cells were sealed with the glass sealant developed at Ceramatec.

Air was supplied directly to the cathode side. Water moistened (at ~30 °C) hydrogen was flowed into the anode side as the fuel at a rate of 81 cm^3/min. Fuel cell tests were automated with a computer and performed from 600 to 800 °C.

To independently determine the conductivity of the LSGM electrolyte used, a long rectangular bar of LSGM was cold pressed with the powders from the same batch of material. It is then sintered at 1550 °C for 6 h. The width and the height of the polished bar were 0.522 and 0.466 cm, respectively. Platinum paste was applied to the two ends and two sections of the bar 1.86 cm apart. Four probe d.c. measurements on its conductivity were performed manually from 500 to 800 °C with platinum leads.

3. Results

Table 1 lists the measured d.c. conductivity of the LSGM electrolyte bar. The conductivity measured at small current has a lower value than that at a large current, which is possibly due to the baseline potential and Seeback effect. We listed the conductivity obtained at intermediate current (10 mA at 800 °C). Its value of 0.075 S/cm at 800 °C is within the range we have usually obtained with an impedance analyzer for its bulk conductivity (0.065–0.1 S/cm).

In the single cells we tested, large overpotentials at the anode and the cathode were observed. In Fig. 2 are given the

Table 1
LSGM conductivity by four-probe d.c. measurement

Temperature (°C)	800	700	600
Conductivity (S/cm)	0.075	0.0283	0.0061

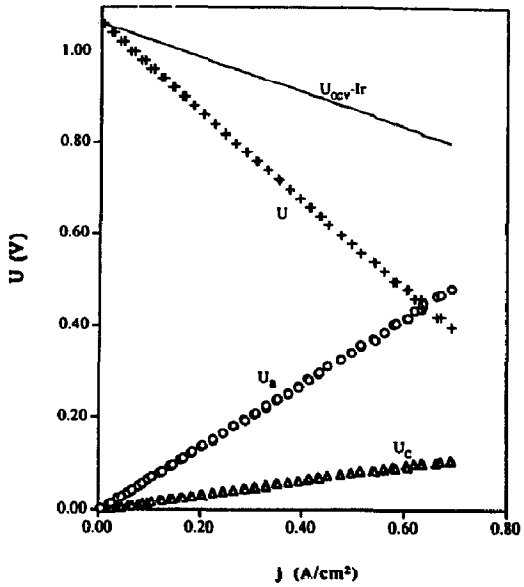

Fig. 2. Potentials of an LSGM single cell at 800 °C with Ni/ceria anode: U is the load potential, U_a is the potential difference between the anode and its reference electrode, U_c is the corresponding quantity for cathode, U_{OCV}–Ir is the load potential without electrode overpotential (assuming an electrolyte conductivity of 0.07 S/cm).

potentials of the cell with ceria/Ni anode measured at 800 °C, in which U is the potential on the load, U_a is the potential difference between its anode and the reference on the anode side, and U_c is that between the cathode and the reference on the cathode side. The contribution of U_a and U_c obeys the following rule

$$U_a + U_c = \eta_a + \eta_c + Ir - \Delta \quad (1)$$

where η_a and η_c are the overpotentials due to the anode and the cathode, respectively, I is the electric current drawn, r is the electrolyte resistance, and Δ is the potential drop between the reference electrodes from the open-circuit potential (OCP). On high cell currents at elevated temperatures, there exist leak currents between the reference electrodes and their working electrodes due to their closeness on the electrolyte surfaces and the high conductivity of the electrolyte. To compare the electrode overpotentials to the potential loss from electrolyte resistance, we plotted the cell potential due solely to the internal resistance assuming no electrode overpotentials in a dashed line, U_{OCV}–Ir. r is calculated from the electrolyte conductivity obtained with our four-probe measurement, 0.07 S/cm. U_a is over three times larger than U_c, and their sum is more than twice the calculated potential drop due to the electrolyte, i.e. Ir. The loss of the electromotive force due to the overpotentials on the electrodes is twice as large as that due to the internal resistance of the oxide-ion electrolyte. Hence, the maximum power density generated by the fuel cell at 800 °C is only about 39% of its theoretical maximum, 0.75 W/cm^2 (thickness: 265 μm, σ: 0.07 S/cm, OCV: 1.064 V). Fig. 3 displays the power density of this cell from 700 to 800 °C. At lower temperatures, overpotentials

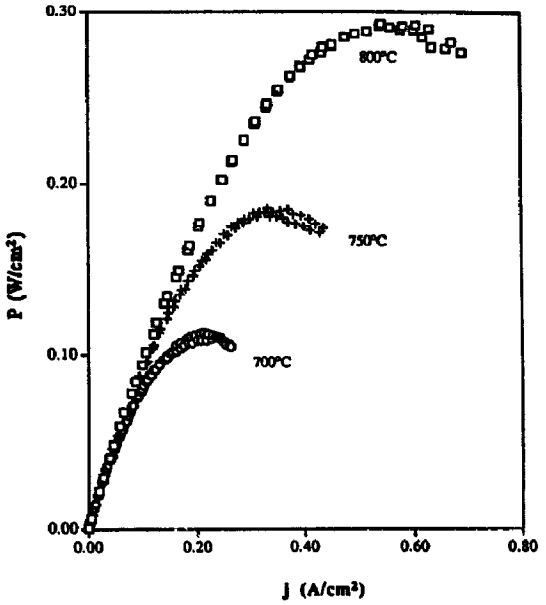

Fig. 3. Power density of an LSGM single cell with Ni/ceria anode at three operating temperatures.

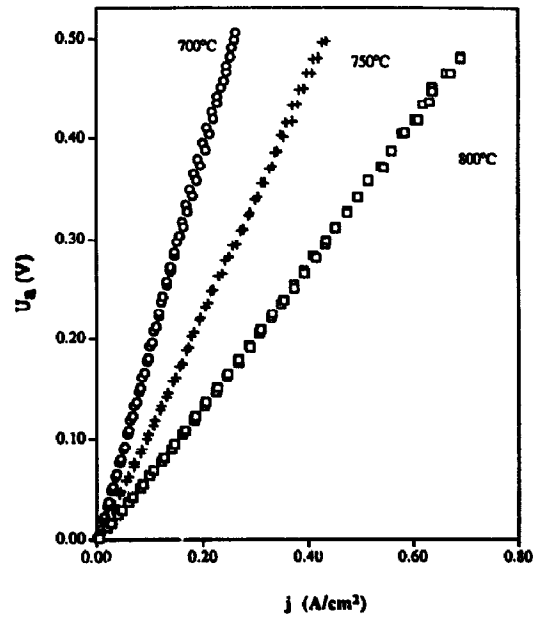

Fig. 4. Anode potential drop U_a of an LSGM single cell with Ni/ceria anode at three operating temperatures.

from the electrodes are even more dominant. At 700 °C, the sum of U_a and U_c is about three times the potential drop from the electrolyte estimated with a conductivity of 0.028 S/cm. This is primarily due to the lower fuel and oxygen reaction rate at the two electrode surfaces at low operating temperatures. Figs. 4 and 5 plot the measured U_a and U_c of this cell at three operating temperatures.

After 11 h of operation, the performance of the single cell with ceria/Ni anode showed slight improvement. The maximum power density increased by about 5%. No significant change in cathode overpotentials was observed. The potential

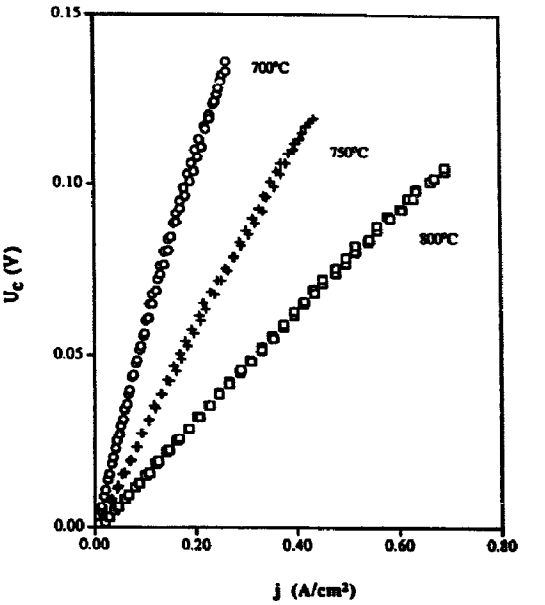

Fig. 5. Cathode potential drop U_c of an LSGM single cell with Ni/ceria anode at three operating temperatures.

drop between the anode and its reference electrode, U_a, decreased by about 50%. However, we found U_a+U_c+U significantly lower than the OCV at the maximum power density current near 0.6 A/cm² (as much as 0.264 V versus a maximum of 0.105 V for the first test). The electrode configurations were not optimized and the origin of the losses were not identified. The data show clearly that not all the drop in U_a originated from the decrease in anode overpotential η_a. As the true OCV was not changed, the decrease in U_a may be due to the smearing of the anode and its reference electrode. The true change in anode overpotential η_a may be only marginal.

We also studied carefully the cell performance with the LSGM/Ni anode. Contrary to the previous one, this cell showed deterioration in performance with time (see second test). Fig. 6 plots the power density from two measurements at 800 °C about 20 h apart. The maximum power density from the first test is about 0.363 W/cm², which is 70% of the theoretical value 0.517 W/cm² (thickness: 395 μm, electrolyte conductivity: 0.07 S/cm, OCV: 1.08 V). A small increase in its OCV suggests a better seal of the cell was achieved. Compared with the cell with an Ni/ceria anode, this cell has an anode potential drop U_a of about 50% smaller, and a cathode potential difference U_c of about 100% increase at the same current density, which may reflect the smaller electrode area. This finding suggests a possible reduction of the large anode overpotential observed in the cell with a ceria/Ni anode. The sum of U_a and U_c of this cell is 20% less than that of the Ni/ceria cell at its maximum powder density. The possible cause of the improvement at the anode side may be due to a better lattice match at the interface and the slightly higher oxide-ion conductivity of the LSGM material over that of ceria. Due to an excess amount of glass sealant applied

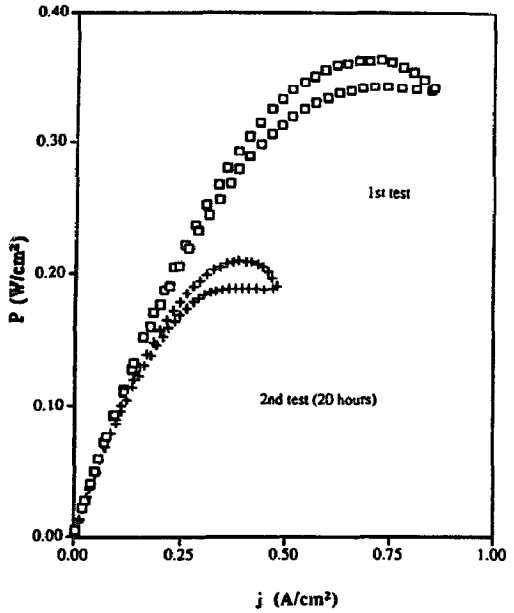

Fig. 6. Power density of two tests at 800 °C for the cell with Ni/LSGM anode.

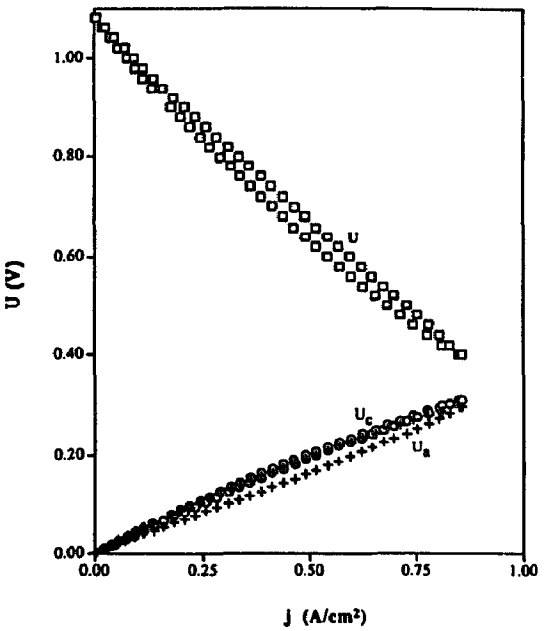

Fig. 7. Potentials from the first test at 800 °C for the cell with Ni/LSGM anode.

at the cathode side, the sealant overflowed the cathode surface after its curing and may have reacted with lanthanum cobaltite to give the higher cathode overpotential. Fig. 7 plotted the potential drop at both the cathode and the anode together with the load potential. The potential drop is almost in equal amount at the two electrodes.

A second test on the cell with the LSGM/Ni anode found a much smaller maximum power density, 0.209 W/cm^2, which is only about 40% of its theoretical value. The anode potential drop U_a in the second test increased 100% over that of the first test at the same current density, while that of the cathode potential drop U_c only showed a slight deterioration. The primary cause of this deterioration is unknown. It has been shown that the ratio of the particle sizes in yttria stabilized zirconium/Ni or ceria/Ni anodes and their morphology have a great impact on the electrochemical performance of the electrode. Moreover, nickel coarsening (or sintering) during fabrication and operation results in loss of active surface area and reduces the conductivity of the anode, leading to a degradation of cell performance with time. The building of a ceria or LSGM network that not only supports a fine dispersion of the Ni particles, but also inhibits their migration and coalescence into large particles, is a critical factor in anode design.

4. Discussion

Single cell tests using doped lanthanum gallate electrolyte material were performed in the temperature range from 600 to 800 °C. Although different geometrical dimension of the electrolyte membranes and two anode supporting material (doped ceria, and electrolyte material LSGM) were used for the two cells, the steady maximum power density achieved were all about 40% of their theoretical values. Four probe d.c. measurements on the same batch of LSGM material together with a large OCV confirmed high oxide-ion conductivity (0.075 S/cm at 800 °C) for the electrolyte. The low performance of the cells originates from the large overpotentials at both the anode and the cathode of the cells. The energy exhausted on the electrodes is larger than that lost due to the resistance of the electrolyte material. A significant deterioration in the maximum output power from 70 to 40% of its theoretical value over time in the cell with a composite LSGM/Ni anode may simply be an artifact of a particular experiment. However, uncertainty remains as to the most suitable supporting material and processing procedure of the anode for a fuel cell with the LSGM electrolyte material.

In light of our test results, identifying a suitable anode supporting material to achieve lower electrode overpotential is the key to the success of the fuel cell with the LSGM electrolyte material. A mixed oxide-ion and electron conductor in perovskite structure and stable in reducing atmosphere is the prime choice. Such materials do exist, including doped $SrCeO_3$, $BaCeO_3$ and $BaIn_{1-x}Ti_xO_{3-\delta}$. The proton conduction in these material partially suppresses the oxide-ion conduction, but may offer a better catalytic ability for the oxidation of humid hydrogen. Also, doped ceria does have a good mixed conductivity. Its different crystal structure from the perovskite LSGM and the higher sintering temperature of ceria pose a problem to achieve good cohesion as a supporting electrode to the LSGM electrolyte. Detailed study on the processing method is necessary. No systematic study on the LSGM as the supporting material for an anode has been reported, possibly due to its lack of any significant electronic conductivity even in pure hydrogen atmosphere. However,

the initial high performance of our cell with this material as the anode support suggests its potential to be the best compatible anode material. The prime merits are its identity to the electrolyte and one of the highest oxide-ion conductor in a reducing atmosphere. The relatively lower sintering temperature during anode fabrication (1400 °C) of the LSGM ceramics over that of ceria can achieve good adhesion to the electrolyte. Sol–gel prepared LSGM may be used as the initial testing material for the anode support. In short, the success of LSGM electrolyte as the candidate fuel cell material relies on the identification of the right anode material and processing methods.

Acknowledgements

We thank the Electric Power Research Institute (EPRI) for financial support and for their interest in the progress of the work. One of us, Man Feng, would also like to express his gratitude to the K.C. Wong Education Foundation, Hong Kong for its sponsorship of his research program at the University of Texas at Austin.

References

[1] A.V. Strelkov, A.R. Kaul, Yu.D. Tretyakov, M. Balkanski, T. Takahashi and H.L. Tuller (eds.), *Solid State Ionics, Proc. Symp. Solid State Ionics of the Int. Conf. on Advanced Materials, May 1991*, Elsevier, Amsterdam, 1992, p. 605.

[2] T. Ishihara, H. Matruda and Y. Takita, *J. Am. Chem. Soc., 116* (1994) 3801.

[3] M. Feng and J.B. Goodenough, *Eur. J. Solid State Inorg. Chem., 31* (1994) 663.

[4] M. Feng, J.B. Goodenough and K. Huang, Sol–gel preparation of doped $LaGaO_3$, *Proc. 1st. Scientific Workshop for Electrochemical Materials, Osaka, Japan, Jan. 1996*, p. 87.